Front. Phys. China, 2009, 4(3): 383–388
DOI 10.1007/s11467-009-0028-4

RESEARCH ARTICLE

Electronic properties of boron nanotubes with axial strain

Yi DING (丁一), **Jun NI** (倪军)(✉)

Department of Physics and Key Laboratory of Atomic and Molecular Nanoscience (Ministry of Education), Tsinghua University, Beijing 100084, China

E-mail: junni@mail.tsinghua.edu.cn

Received January 17, 2009; accepted February 20, 2009

The electronic properties of boron nanotubes with axial strain are investigated by first principle calculations. The band gaps of the (3, 3) and (5, 0) boron nanotubes are found to be modified by axial strain significantly. We find that the semiconductor–metal transition occurs for the (3, 3) boron nanotubes with both compressive and tensile strain. While for the (5, 0) boron nanotubes, only the tensile strain induces the semiconductor–metal transition. These boron nanotubes have the largest gaps under compressive strain.

Keywords boron nanotube, strain, electronic structure, band gap

PACS numbers 68.65.-k, 73.22.-f, 73.63.Fg, 81.07.De

1 Introduction

One-dimensional nano-materials, such as carbon nanotubes and graphene nanoribbons, have attracted a lot of experimental and theoretical attention [1−6]. For single-walled carbon nanotubes, they can be semiconductors or metals depending on the chirality and size [1]. While for graphene nanoribbons, the shape of edges play the most important role in the electronic properties [2]. Due to the unique electronic structures, carbon nanotubes and graphene nanoribbons have been used in nanoscale semiconductor devices [3, 4]. The one-dimensional nano materials are not limited to carbon-based materials. The inorganic nanotubes, such as WS_2 and MoS_2, have been reported to be synthesized by making use of solid templates [5]. New synthetic strategies for the formation of inorganic nanotubes have been developed, by which high-quality semiconductor nanotubes have been produced [6].

Boron is the left neighbor of carbon in the periodic table. Ciuparu *et al.* reported the synthesis of single-walled boron nanotubes with diameters in the range of 3 nm [7]. Recently, Szwacki *et al.* have predicted that the boron buckyball B_{80} was a stable hollow cage, which is symmetrically similar to the C_{60} structure [8]. The B_{80} can form stable face-centered-cubic and body-centered-cubic solids, both of which are metals [9, 10]. A flat stable boron sheet has been predicted, which is composed of a hybrid of triangular and hexagonal configuration [11, 12]. By first principles calculations, the vibrational frequency, free energy, and heat capacity of the flat hybridized sheet and buckled triangular sheet are compared to verify the thermodynamic stability of the flat boron sheet [13].

Using the stable flat boron sheet as precursors, a series of single-walled boron nanotubes (SWBNTs) [12, 14, 15] and nanoribbons [16] were obtained. For SWBNTs, they can be semiconductors or metals depending mainly on the size of the tubes [12, 14]. When the diameters of the tubes are larger than 17 Å, all the SWBNTs become metals regardless of chirality [12, 14]. For the boron nanoribbons, they can be semiconductors or metals depending on the number of hydrogen passivated on the zigzag edges. The bare boron nanoribbons and one-hydrogen passivated ones are metals, while the two-hydrogen passivated ones become semiconductors, if the width is less than 24 Å [16].

The electronic properties of one-dimensional nanotubes are distinct for applications. By chemical modification, carbon nanotubes have better electronic, optical, thermal and mechanical properties than those of the pure carbon counterparts [17]. Besides the doping effects, the strain is usually used to tuning the electronic properties of nano-structures [18−22]. Under axial strain, a semiconductor–metal transition is predicted to occur in all zigzag single-wall carbon nanotubes [18]. For the (n, 0) semiconducting single-wall carbon nanotubes, the gaps with strain vary with the change of n: when

$mod(n,3) = 1$, the strain-induced gap increases while when $mod(n,3) = 2$, the strain-induced gap decreases [19]. Using an atomic force microscope tip to vary the carbon nanotube strain, Minot *et al.* found that strain can open a band gap in a metallic nanotube and modify the band gap in a semiconducting nanotube [20]. For the graphene nanoribbons, the band gaps of zigzag nanoribbons are not sensitive to axial strain, while the band gaps of armchair nanoribbons varies as a function of axial strain [21]. Besides carbon-based materials, strain is also used to control the electronic band structure of Si nanowires, which are manipulated to have direct band gaps of Si nanowires by applying lattice strain [22]. Recently, single-crystalline boron nanowires have been synthesized in experiments [23, 24]. Tensile stress measurements demonstrated that the prepared boron nanowire has excellent mechanical properties as well as resistance to mechanical fracture even under a strain of 3% [24]. Although the boron nanowires experimentally synthesized are structurally different to the SWBNTs, a theoretical study of strain effects on the SWBNTs will provide insightful information for the experimental findings.

In this paper, we investigate the electronic properties of boron nanotubes with axial strain by first principle calculations. The semiconducting boron nanotube such as (3, 3) and (5, 0) SWBNTs [12, 14, 15] are studied. For both SWBNTs, the band gaps are found to be modified by axial strain significantly. For the (3, 3) SWBNTs, the semiconductor–metal transition occurs with compressive and tensile strain less than 7.5%. While for the (5, 0) SWBNTs, only the tensile strain induces semiconductor–metal transition when the tension is up to 8% strain.

2 Methods

First principles calculations are performed by the SIESTA (Spanish Initiative for Electronic Simulations with Thousands of Atoms) code [25]. The total energies and electronic structures are calculated within the density-functional theory using a double-ζ basis set with additional orbitals of polarization. In our calculations, the local density approximation (LDA) is adopted for the exchange-correlation functional and the Troullier-Martins scheme is used for the norm-conserving pseudopotentials. A grid cutoff of 175 Ry is used and the Brillouin zone sampling is done using a $1\times1\times15$ Monkhorst-Pack grid. The supercells are used to simulate the isolated SWBNTs and SWBNTs are parallel to the z axis. The distance of SWBNTs is larger than 10 Å in order to avoid interactions. All the structures are relaxed until the maximum atomic force is smaller than 0.04 eV/Å.

We perform the variable-cell calculations to get the optimized lattice constants for the SWBNTs without strain. For the (3, 3) SWBNTs, the equilibrium length Z_0 in the axial direction of the unit cell is 5.07 Å. For the (5, 0) SWBNTs, we obtain $Z_0 = 8.76$ Å. The axial strain is given by changing the unit cell size along the axial direction. After changing the lattice length, the coordinates of boron atoms are relaxed to obtain their equilibrium positions. Then the electronic structures and strain energies are calculated for the SWBNTs with axial strain. In our paper, the axial strain is expressed as

$$\epsilon = (Z - Z_0)/Z_0$$

where Z is the corresponding length of the unit cell for the strained SWBNTs. Negative ϵ value corresponds to compressive strain and positive ϵ value corresponds to tensile strain.

3 Results

The electronic properties of the (3, 3) SWBNTs under different strain are shown in Figure 1. For the nanotube without strain, we obtain an LDA band gap of 0.215 eV, which is in accordance with previous studies [12, 14]. The (3, 3) SWBNTs have a direct band gap and the valence band maximum (VBM) and conduction band minimum (CBM) are at the Γ point. When the compression is applied to the (3, 3) SWBNTs, the conduction bands drop down near the X point and the position of CBM changes from the Γ point to $kd_Z \approx 4/5$ point. On the other hand, the position of VBM stays at the Γ point for the (3, 3) SWBNTs with compressive strain. At the strain of $\epsilon = -2.5\%$, the minimum values of conduction bands at the Γ point and $kd_Z \approx 4/5$ point are nearly the same as shown in Fig. 1(c). When the strain is up to $\epsilon = -5.0\%$, the CBM is located at the $kd_Z \approx 4/5$ point, and the (3, 3) SWBNTs have an indirect band gap of 0.131 eV. When the strain are $\epsilon = -7.5\%$, the conduction bands near the $kd_Z \approx 4/5$ point drop below the Fermi level and the (3, 3) SWBNTs become metals as shown in Fig. 1(a).

When the tension is applied to the (3, 3) SWBNTs, the position of CBM stays at the Γ point while the position of VBM changes from the Γ point to $kd_Z \approx 1/3$ point. When the strain reaches $\epsilon = 2.5\%$, the minimum values of conduction bands at the Γ point and $kd_Z \approx 1/3$ point are nearly the same as shown in Fig. 1(e). When the strain is up to $\epsilon = 5.0\%$, the valence bands near the $kd_Z \approx 1/3$ point rise to the Fermi level. The conduction bands drop below the Fermi level and the (3, 3) SWBNTs become metals as shown in Fig. 1(f). As the strain increases to $\epsilon = 7.5\%$, the (3, 3) SWBNTs maintains metallicity.

The band gaps as a function of the strain ϵ is plotted in Fig. 2(a). Under the tensile strain, the (3, 3) SWBNTs have smaller band gaps than the ones without strain. The semiconductor–metal transition occurs

at $\epsilon = 4.0\%$. For a larger tensile strain, the (3, 3) SWBNTs are always metals. When the compressive strain is applied to the (3, 3) SWBNTs, the band gaps increase first. When $\epsilon = -2.0\%$, the (3, 3) SWBNTs have the largest band gap of 0.295 eV. Then the band gap decreases with the increase of compressive strain. The semiconductor–metal transition occurs at $\epsilon = -6.0\%$. The strain energies of the (3, 3) SWBNTs, which are denoted as $\Delta E = E(\epsilon) - E(0)$, are shown in Fig. 2(b). Here, $E(\epsilon)$ is the total energy of the strained SWBNTs and $E(0)$ is the total energy of the nanotubes without strain. The strain energies ΔE as a function of ϵ is a parabolic curve. The metallic (3, 3) SWBNTs with $\epsilon = 4.0\%$ are 27 meV per boron atom in energy higher than the ones without strain, while the strain energies of metallic ones with $\epsilon = -6.0\%$ are 76 meV per boron atom. Thus, the (3, 3) SWBNTs change to metals more easily with tension than compression.

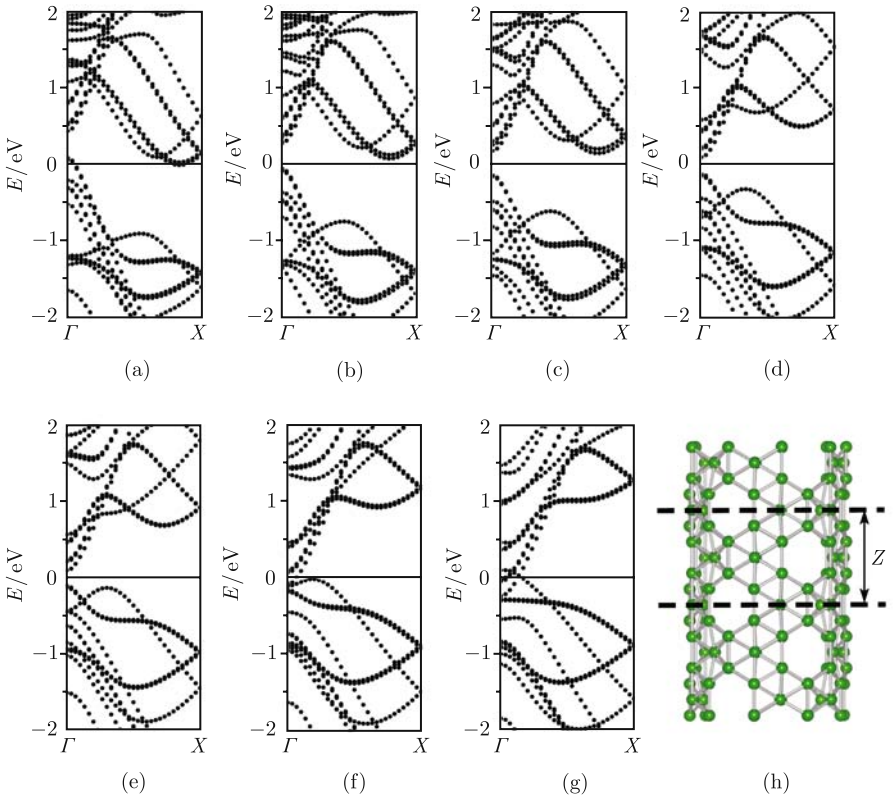

Fig. 1 The band structures of the (3, 3) SWBNTs under axial strain at **(a)** $\epsilon = -7.5\%$, **(b)** $\epsilon = -5.0\%$, **(c)** $\epsilon = -2.5\%$, **(d)** $\epsilon = -0.0\%$, **(e)** $\epsilon = 2.5\%$, **(f)** $\epsilon = 5.0\%$, **(g)** $\epsilon = 7.5\%$. The structure of the (3, 3) tube is shown in **(h)**. The Fermi level is indicated as the line at $E = 0.0$ eV.

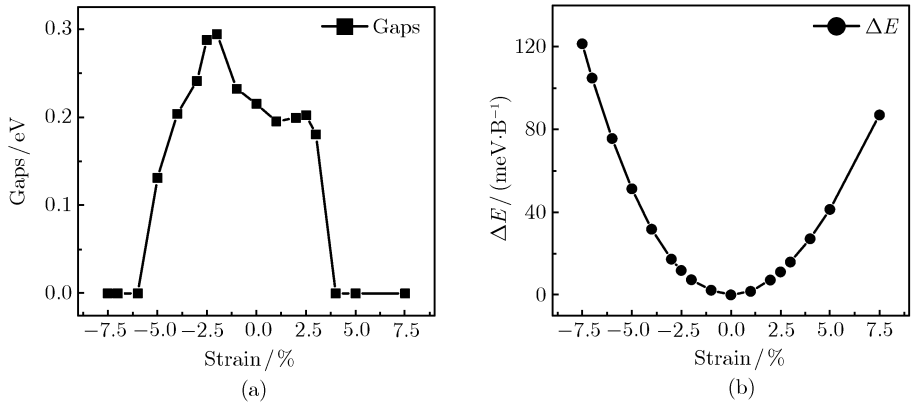

Fig. 2 **(a)** The band gaps and **(b)** the strain energies of the (3, 3) SWBNTs as functions of strain.

For the (5, 0) SWBNTs, the electronic structures under different strain are shown in Fig. 3. The (5, 0) SWBNTs without strain have an indirect band gap of 0.650 eV, which also agrees with previous studies [12, 14]. The CBM is located at the $kd_Z \approx 4/5$ point and the VBM is located at the $kd_Z \approx 2/5$ point. When the compression is applied to the (5, 0) SWBNTs, one conduction band at the Γ point becomes lower significantly and the valence bands at the Γ point also change. When the compressive strain is $\epsilon = -7.5\%$, the position of CBM changes to Γ point and the VBM moves to the $kd_Z \approx 1/3$ points. As shown in Fig. 3(a), the (5, 0) SWBNTs with $\epsilon = -7.5\%$ is semiconducting with a gap of 0.325 eV. When the strain increase to $\epsilon = -10.0\%$, the structure cannot keep a tube form after relaxation. Thus, we find that (5, 0) SWBNTs have no semiconductor–metal transition under compressive strain.

For the (5, 0) SWBNTs with tensile strain, the conduction bands at the Γ points become lower significantly. The CBM is located at the Γ points for ϵ=2.5%. Under the tensile strain ϵ=7.5%, the band gap decreases to 0.116 eV as shown in Fig. 3(g). When the strain increases, the structure maintains a tube form and semiconductor–metal transition occurs as shown in Fig. 4(a).

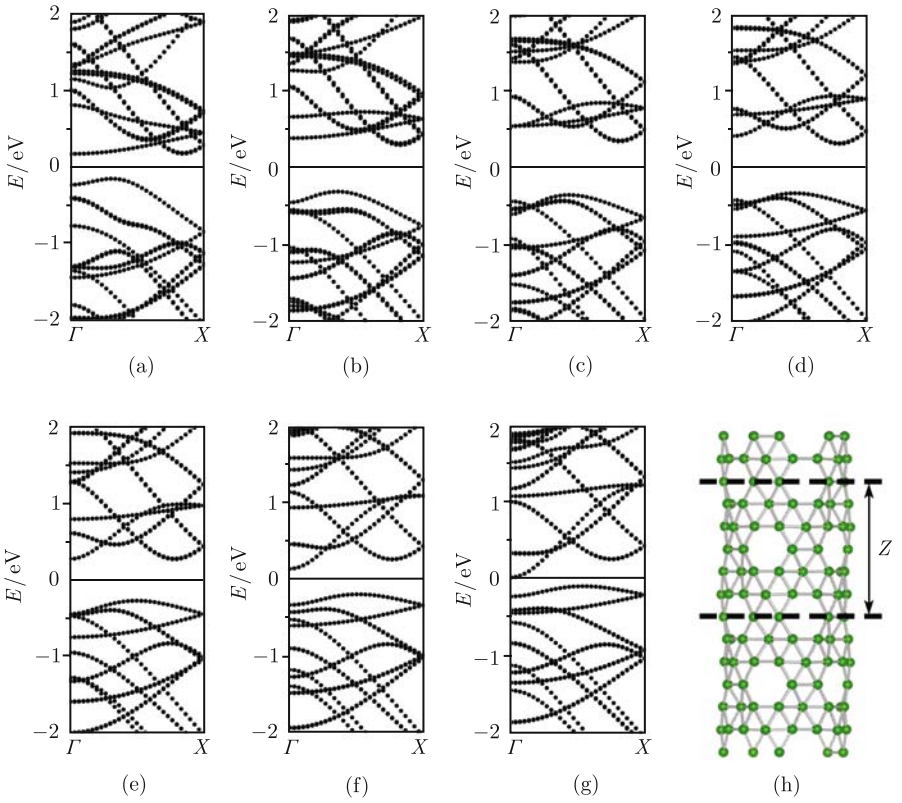

Fig. 3 The band structures of the (5, 0) SWBNTs under axial strain at **(a)** $\epsilon = -7.5\%$, **(b)** $\epsilon = -5.0\%$, **(c)** $\epsilon = -2.5\%$, **(d)** $\epsilon = -0.0\%$, **(e)** $\epsilon = 2.5\%$, **(f)** $\epsilon = 5.0\%$, **(g)** $\epsilon = 7.5\%$. The structure of the (5, 0) tube is shown in **(h)**. The Fermi level is indicated as the line at $E = 0.0$ eV.

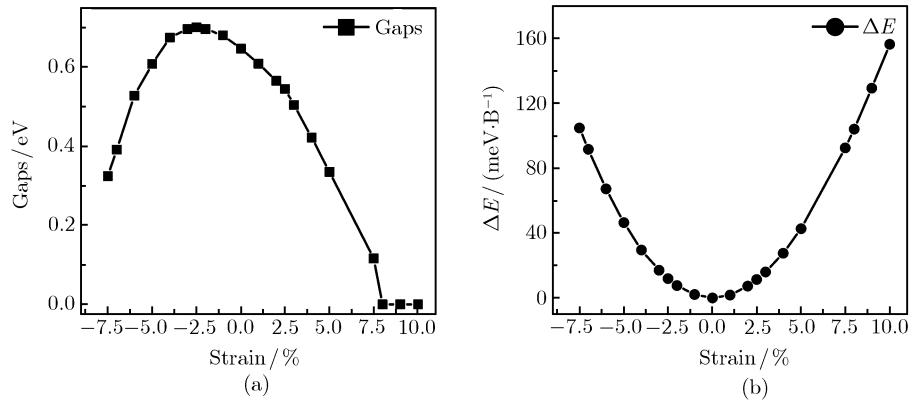

Fig. 4 **(a)** The band gaps and **(b)** the strain energies of the (5, 0) SWBNTs as functions of strain.

We plot the variation of the band gap for the (5, 0) SWBNTs under strain in Fig. 4(a). The variation of the band gap for strained (5, 0) SWBNTs is similar to that of the (3, 3) ones. Under the tensile strain, the band gap decreases monotonously and the (5, 0) SWBNTs become metals at $\epsilon = 8.0\%$. Under the compressive strain, the band gap increases first and then decreases monotonously. At $\epsilon = -2.5\%$, the (5, 0) SWBNTs have the largest band gap of 0.702 eV. However, different from the (3, 3) SWBNTs, there is no semiconductor–metal transition for the (5, 0) nanotubes under compression. The strain energies of the (5, 0) SWBNTs are shown in Fig. 4(b). The metallic (5, 0) SWBNTs with $\epsilon = 8.0\%$ are 104 meV per boron atom in energy higher than the ones without strain. Thus, it is hard for the (5, 0) SWBNTs to become metals under axial strain.

The (3, 3) and (5, 0) boron nanotubes open the band gaps due to rehybridization of buckled boron atom [14]. The semiconductor–metal transitions occur when the rehybridization is broken. We plot the local density of states (LDOS) of the (3, 3) and (5, 0) SWBNTs in Fig. 5 and 6, respectively. For the (3, 3) SWBNTs, the LDOSs of VBM and CBM for strained nanotube at $\epsilon = -2.0\%$, which have the largest band gap in the calculated range, are shown in Fig. 5 (a) and (b) with a broadening factor of 0.1 eV. The LDOSs of VBM and CBM for the strained (3, 3) SWBNTs have similar shape as the HOMO and LUMO of B_{80} [26]. While for the metallic nanotubes, the LDOSs at Fermi level are quite different from those for the semiconducting ones. For the compression, the tube form change from cylinder to hexagon prism. While for the tension, the buckling of the boron atoms weaken as shown in Fig. 5(d). Thus, the strain breaks the buckling and the rehybridization disappears when the semiconductor–metal transitions occur. The same mechanism exists in the strained (5, 0) SWBNTs. The LDOS of VBM for the strained nanotubes ($\epsilon = -2.0\%$) in Fig. 6 has a similar shape as those for the nanotubes without strain [14]. When the compressive strain is applied, the rehybridization remains as shown in Fig. 6(c) and the nanotubes are always semiconducting. While for the tensile strain, as the unit cell length along the z axis increases, the buckling of the boron atoms weaken and the rehybridization disappears. Thus, the semiconductor–metal transition appears for the (5, 0) SWBNTs under tension.

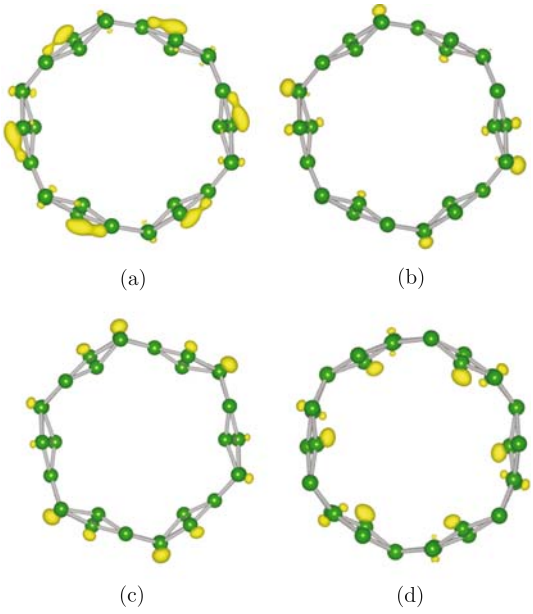

Fig. 5 The LDOSs of the (3, 3) SWBNTs for **(a)** VBM with $\epsilon = -2.0\%$, **(b)** CBM with $\epsilon = -2.0\%$, **(c)** around the Fermi energy level with $\epsilon = -7.5\%$, **(d)** around the Fermi energy level with $\epsilon = 7.5\%$. The isosurfaces are 50% of the maximum of the density.

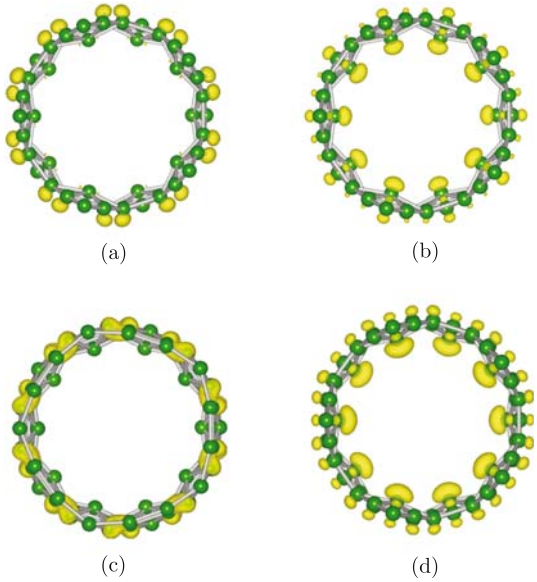

Fig. 6 The LDOSs of the (5, 0) SWBNTs for **(a)** VBM with $\epsilon = -2.0\%$, **(b)** CBM with $\epsilon = -2.0\%$, **(c)** VBM with $\epsilon = -7.5\%$, **(d)** CBM with $\epsilon = 7.5\%$. The isosurfaces are 50% of the maximum of the density.

4 Conclusion

We have studied the electronic structure of (3, 3) and (5, 0) SWBNTs under axial strain. The band gaps of both SWBNTs are modified by the compressive and tensile strain. Both (3, 3) and (5, 0) SWBNTs have the largest gap values under about 2% and 2.5% compressive strain. The semiconductor–metal transitions occur for the (3, 3) SWBNTs at compressive strain $\epsilon = -6.0\%$ and tensile strain $\epsilon = 4.0\%$. For the (5, 0) SWBNTs, the tensile strain of up to $\epsilon = 8.0\%$ induces semiconductor–metal transition. The semiconductor–metal transitions occur due to the strain weakening the buckling of boron nanotubes and breaking the rehybridization.

Acknowledgements This research was supported by the National Natural Science Foundation of China (Grant Nos. 10674076 and 10721404) and the Ministry of Science and Technology of China (Grant No. 2006CB605105).

References

1. J. C. Charlier, X. Blase, and S. Roche, Rev. Mod. Phys., 2007, 79: 677
2. A. H. Castro Neto, F. Guinea, N. M. R. Peres, K. S. Novoselov, and A. K Geim, arXiv: 0709.1163v2
3. M. Endo, M. S. Strano, and P. M. Ajayan, Carbon Nanotubes, Topics Appl. Phys., Springer Press, 2008, 111: 13
4. P. Avouris, Z. H. Chen, and V. Perebeinos, Nature Nanotechnology, 2007, 2: 605
5. R. Tenne, Nature Nanotechnology, 2006, 1: 103
6. C. L. Yan, J. Liu, F. Liu, J. S. Wu, K. Gao, and D. F. Xue, Nanoscale Res. Lett., 2008, 3: 473
7. D. Ciuparu, R. F. Klie, Y. Zhu, and L. Pfefferle, J. Phys. Chem. B, 2004, 108: 3967
8. N. G. Szwacki, A. Sadrzadeh, and B. I. Yakobson, Phys. Rev. Lett., 2007, 98: 166804-1
9. Q. B. Yan, Q. R. Zheng, and G. Su, Phys. Rev. B, 2008, 77: 224106-1
10. A. Y. Liu, R. R. Zope, and M. R. Pederson, Phys. Rev. B, 2008, 78: 155422-1
11. H. Tang and S. Ismail-Beigi, Phys. Rev. Lett., 2007, 99: 115501-1
12. X. Yang, Y. Ding, and J. Ni, Phys. Rev. B, 2008, 77: 041402(R)-1
13. K. C Lau and R. Pandey, J. Phys. Chem. B, 2008, 112: 10217
14. A. K. Singh, A. Sadrzadeh, and B. I. Yakobson, Nano Lett., 2008, 8: 1314
15. L. A. Chernozatonskii, P. B. Sorokin, and B. I. Yakobson, JETP Lett., 2008, 87: 489
16. Y. Ding, X. Yang, and J. Ni, Appl. Phys. Lett., 2008, 93: 043107-1
17. S. Singh and P. Kruse, Int. J. Nanotechnol., 2008, 5: 900
18. S. Sreekala, X. H. Peng, P. M. Ajayan, and S. K. Nayak, Phys. Rev. B, 2008, 77: 155434-1
19. P. K. Valavala, D. Banyai, M. Seel, and R. Pati, Phys. Rev. B, 2008, 78: 235430-1
20. E. D. Minot, Y. Yaish, V. Sazonova, J. Y. Park, M. Brink, and P. L. McEuen, Phys. Rev. Lett., 2003, 90: 156401-1
21. L. Sun, Q. Li, H. Ren, H. Su, Q. W. Shi, and J. Yang, J. Chem. Phys., 2008, 129: 074704-1
22. K. H. Hong, J. Kim, S. H. Lee, and J. K. Shin, Nano Lett., 2008, 8: 1335
23. F. Liu, J. Tian, L. Bao, T. Yang, C. Shen, X. Lai, Z. Xiao, W. Xie, S. Deng, J. Chen, J. She, N. Xu, and H. Gao, Adv. Mater., 2008, 20: 2609
24. J Tian. J. Cai, C. Hui, C. Zhang, L. Bao, M. Gao, C. Shen, and H. Gao, Appl. Phys. Lett., 2008, 93: 122105-1
25. J. M. Soler, E. Artacho, J. D. Gale, A. García, J. Junquera, P. Ordejo, and D. Sánchez-Portal, J. Phys.: Condens. Matter, 2002, 14: 2745
26. T. Baruah, M. R. Pederson, and R. R. Zope, Phys. Rev. B, 2008, 78: 045408-1